May 6, 2013

Microscopic origin of the nucleon-nucleon interaction

Since the nucleon-nucleon interaction is a short-range force, Yukawa proposed, in analogy to the one-photon exchange in electrodynamics, a massive-particle (boson) exchange interaction in 1935. In QED, the Coulomb interaction is mediated by a field of zero mass particles, the photons. In the static approximation, the potential satisfies the Poisson equation

$$-\Delta V(\vec{r}) = e\,\delta^{(3)}(\vec{r})$$

with the Coulomb potential as solution $V(r) = \frac{e}{4\pi}\frac{1}{r}$.

If the exchange particles are massive (and the nucleons are infinitely heavy and fixed at the origin), the corresponding potential satisfies

$$\left(-\Delta + m^2\right)\varphi(\vec{r}) = g\,\delta^{(3)}(\vec{r})$$

with the Yukawa potential as solution $\varphi(r) = \frac{g}{4\pi}\frac{e^{-mr}}{r}$

In relativistic quantum field theory, Yukawa potentials are derived from a one-boson exchange amplitude. In the center-of-mass frame

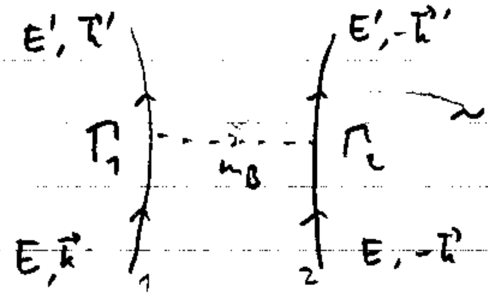

$$\sim \frac{1}{(k-k')^2 - m_B^2}$$

4-vectors

where Γ_i denote the spin-structure of the vertex, e.g., for

pseudoscalar bosons $\mathcal{L}_{ps} = -g_{ps}\bar{\Psi}\underbrace{i\gamma_5}_{\Gamma^{(ps)}}\Psi\varphi^{(ps)}$

scalar bosons $\mathcal{L}_s = \underbrace{+g_s}_{\Gamma^{(s)}}\bar{\Psi}\Psi\varphi^{(s)}$

vector bosons (e.g., photon $\varphi_\mu^{(v)} = A_\mu$) and $m_B = 0$

$\mathcal{L}_v = -g_v\bar{\Psi}\underbrace{\gamma^\mu}_{\Gamma^{(v)}}\Psi\varphi_\mu^{(v)}$

$- \frac{f_v}{4m_N}\bar{\Psi}\sigma^{\mu\nu}\Psi\left(\partial_\mu\varphi_\nu^{(v)} - \partial_\nu\varphi_\mu^{(v)}\right)$

Ψ are the nucleon fields and $\varphi^{(i)}$ the mesonic boson fields. Below is a table of the different mesons contributing to the NN interaction and their importance (strong/weak) and nature (attraction/repulsion).

TABLE 3.1

Various Meson–Nucleon Couplings and their Contributions to the Nuclear Force as Obtained from One-Boson Exchange

I denotes the isospin of a boson. The characteristics quoted refer to $I = 0$ bosons (no isospin dependence). The isovector ($I = 1$) boson contributions, carrying a factor $\tau_1 \cdot \tau_2$, provide the isospin-dependent forces.

Coupling	Bosons (Strength of coupling)		Characteristics of predicted forces			
	$I = 0$ [1]	$I = 1$ [$\tau_1 \cdot \tau_2$]	Central [1]	Spin–Spin [$\sigma_1 \cdot \sigma_2$]	Tensor [S_{12}]	Spin-Orbit [$\mathbf{L} \cdot \mathbf{S}$]
ps	η (weak)	"pion" π (strong)	—	Weak, coherent with *v*, *t*	Strong	—
s	"sigma" σ (strong)	δ (weak)	Strong, attractive	—	—	Coherent with *v*
v	"omega" ω (strong)	"rho" ρ (weak)	Strong, repulsive	Weak coherent with *ps*	Opposite to *ps*	Strong, coherent with *s*
t	ω (weak)	ρ (strong)	—	Weak, coherent with *ps*	Opposite to *ps*	—

The amplitude of the one-boson exchange interaction is given relativistically by

additional terms in the propagator, e.g., from ∂_μ in vector boson interactions.

$$\frac{\bar{u}_1(\vec{k}')\,\Gamma_1\, u_1(\vec{k})\; P_B\; \bar{u}_2(-\vec{k}')\,\Gamma_2\, u_2(-\vec{k})}{(k_\mu - k'_\mu)\cdot(k^\mu - k'^\mu) - m_B^2}$$

If one performs a relativistic reduction, i.e., we expand in $\frac{\vec{k},\vec{k}'}{m_N}$ one finds in the static limit:

$= -\vec{q}$ $\qquad\qquad$ $\frac{1}{2}(\vec{\sigma}_1 + \vec{\sigma}_2)$

$= -\vec{q}\,'$

$$V_{ps}(\mathbf{k}) = -\frac{g_{ps}^2}{4M^2}\frac{(\boldsymbol{\sigma}_1\cdot\mathbf{k})(\boldsymbol{\sigma}_2\cdot\mathbf{k})}{\mathbf{k}^2 + m_{ps}^2}$$

$$V_s(\mathbf{k},\mathbf{p}) = -\frac{g_s^2}{\mathbf{k}^2 + m_s^2}\left[1 - \frac{\mathbf{p}^2}{2M^2} + \frac{\mathbf{k}^2}{8M^2} - \underbrace{\frac{i}{2M^2}\mathbf{S}\cdot(\mathbf{k}\times\mathbf{p})}\right]$$

$$\begin{aligned}V_v(\mathbf{k},\mathbf{p}) = \frac{1}{\mathbf{k}^2 + m_v^2}\Bigg\{ & g_v^2\left[1 + \frac{3\mathbf{p}^2}{2M^2} - \frac{\mathbf{k}^2}{8M^2} + \underbrace{\frac{3i}{2M^2}\mathbf{S}\cdot(\mathbf{k}\times\mathbf{p})}\right. \\ & \left. -\boldsymbol{\sigma}_1\cdot\boldsymbol{\sigma}_2\frac{\mathbf{k}^2}{4M^2} + \frac{1}{4M^2}(\boldsymbol{\sigma}_1\cdot\mathbf{k})(\boldsymbol{\sigma}_2\cdot\mathbf{k})\right] \\ & + \frac{g_v f_v}{2M}\left[-\frac{\mathbf{k}^2}{M} + \underbrace{\frac{4i}{M}\mathbf{S}\cdot(\mathbf{k}\times\mathbf{p})} - \boldsymbol{\sigma}_1\cdot\boldsymbol{\sigma}_2\frac{\mathbf{k}^2}{M}\right. \\ & \left. + \frac{1}{M}(\boldsymbol{\sigma}_1\cdot\mathbf{k})(\boldsymbol{\sigma}_2\cdot\mathbf{k})\right] \\ & + \frac{f_v^2}{4M^2}\left[-\boldsymbol{\sigma}_1\cdot\boldsymbol{\sigma}_2\mathbf{k}^2 + (\boldsymbol{\sigma}_1\cdot\mathbf{k})(\boldsymbol{\sigma}_2\cdot\mathbf{k})\right]\Bigg\}\end{aligned}$$

where the $\vec{k}$ here is our $\underbrace{\vec{k}' - \vec{k}}_{-\vec{q}}$ and the $\vec{p}$ is $\underbrace{\frac{1}{2}(\vec{k}' + \vec{k})}_{\vec{q}/2}$

$\Rightarrow$ spin-orbit force is a relativistic effect (higher order in $\frac{\vec{k},\vec{k}'}{m_N}$) and quadratic spin-orbit is of even higher order (don't appear here).

In coordinate space, these correspond to
($S_{12} = 3\, \sigma_1 \cdot \hat{r}\, \sigma_2 \cdot \hat{r} - \sigma_1 \cdot \sigma_2$ and $\nabla^2 = \frac{1}{r} \frac{\partial^2}{\partial r^2} r - \frac{\vec{L}^2}{r^2}$)

The Fourier transform, $V(\mathbf{r}) = (2\pi)^{-3} \int d^3k e^{i\mathbf{k}\cdot\mathbf{r}} V(\mathbf{k})$, which can now be performed analytically, yields [see (Mac 86, Section 3.4) for details]

$$V_{ps}(m_{ps}, \mathbf{r}) = \frac{1}{12} \frac{g_{ps}^2}{4\pi} m_{ps} \left\{ \left(\frac{m_{ps}}{M}\right)^2 \left[Y(m_{ps}r) - \frac{4\pi}{m_{ps}^3} \delta^{(3)}(\mathbf{r}) \right] \boldsymbol{\sigma}_1 \cdot \boldsymbol{\sigma}_2 + Z(m_{ps}\mathbf{r}) S_{12} \right\} \tag{A.20}$$

$$V_s(m_s, \mathbf{r}) = -\frac{g_s^2}{4\pi} m_s \left\{ \left[1 - \tfrac{1}{4} \left(\frac{m_s}{M}\right)^2 \right] Y(m_s r) + \frac{1}{4M^2} [\nabla^2 Y(m_s r) + Y(m_s r) \nabla^2] + \tfrac{1}{2} Z_1(m_s r) \mathbf{L} \cdot \mathbf{S} \right\} \tag{A.21}$$

$$\begin{aligned} V_v(m_v, \mathbf{r}) = \frac{g_v^2}{4\pi} m_v & \left\{ \left[1 + \tfrac{1}{2} \left(\frac{m_v}{M}\right)^2 \right] Y(m_v r) \right. \\ & - \frac{3}{4M^2} [\nabla^2 Y(m_v r) + Y(m_v r) \nabla^2] \\ & \left. + \tfrac{1}{6} \left(\frac{m_v}{M}\right)^2 Y(m_v r) \boldsymbol{\sigma}_1 \cdot \boldsymbol{\sigma}_2 - \tfrac{3}{2} Z_1(m_v r) \mathbf{L} \cdot \mathbf{S} - \tfrac{1}{12} Z(m_v r) S_{12} \right\} \\ & + \tfrac{1}{2} \frac{g_v f_v}{4\pi} m_v \left[\left(\frac{m_v}{M}\right)^2 Y(m_v r) + \tfrac{2}{3} \left(\frac{m_v}{M}\right)^2 Y(m_v r) \boldsymbol{\sigma}_1 \cdot \boldsymbol{\sigma}_2 \right. \\ & \left. - 4 Z_1(m_v r) \mathbf{L} \cdot \mathbf{S} - \tfrac{1}{3} Z(m_v r) S_{12} \right] \\ & + \frac{f_v^2}{4\pi} m_v \left[\tfrac{1}{6} \left(\frac{m_v}{M}\right)^2 Y(m_v r) \boldsymbol{\sigma}_1 \cdot \boldsymbol{\sigma}_2 - \tfrac{1}{12} Z(m_v r) S_{12} \right] \end{aligned} \tag{A.22}$$

with

$$Y(x) = e^{-x}/x \qquad \underline{\text{Yukawa's!}} \tag{A.23}$$

$$Z(x) = \left(\frac{m_\alpha}{M}\right)^2 \left(1 + \frac{3}{x} + \frac{3}{x^2}\right) Y(x) \tag{A.24}$$

$$Z_1(x) = -\left(\frac{m_\alpha}{M}\right)^2 \frac{1}{x} \frac{d}{dx} Y(x) = \left(\frac{m_\alpha}{M}\right)^2 \left(\frac{1}{x} + \frac{1}{x^2}\right) Y(x) \tag{A.25}$$

The Born potential models the NN interaction by several one-boson exchange interactions with the following parameters (masses of the mesons from Particle data)

TABLE A.1

Relativistic OBEP Using the BbS Equation and the *ps* Coupling for π and η

Given are the meson, deuteron, and low-energy parameters. For notation and other information see Tables 4.1 and 4.2. Always used are $f_\rho/g_\rho = 6.1$ and $f_\omega/g_\omega = 0.0$. $n_\alpha = 1$ except $n_\rho = 2$ and $n_\omega(\mathrm{B}) = 2$.

	m_α (MeV)	Potential A		Potential B^a		Potential C	
		$g_\alpha^2/4\pi$	Λ_α (GeV)	$g_\alpha^2/4\pi$	Λ_α (GeV)	$g_\alpha^2/4\pi$	Λ_α (GeV)
π	138.03	14.7	1.3	14.4	1.7	14.2	3.0
η	548.8	4	1.5	3	1.5	0	—
ρ	769	0.86	1.95	0.9	1.85	1.0	1.7
ω	782.6	25	1.35	24.5	1.85	24	1.4
δ	983	1.3	2.0	2.488	2.0	4.722	2.0
σ^b	550	8.8	2.0	8.9437	1.9	8.6289	1.7
	(710–720)	(17.194)	(2.0)	(18.3773)	(2.0)	(17.5667)	(2.0)
$-\varepsilon_d$ (MeV)		2.22452		2.22461		2.22459	
P_D (%)		4.38		4.99		5.61	
Q_d (fm^2)		0.274^c		0.278^c		0.281^c	
μ_d (μ_N)		0.8548^c		0.8514^c		0.8478^c	
A_S (fm$^{-1/2}$)		0.8867		0.8860		0.8850	
D/S		0.0263		0.0264		0.0266	
r_d (fm)		1.9693		1.9688		1.9674	
a_{np} (fm)		−23.750		−23.750		−23.751	
r_{np} (fm)		2.71		2.71		2.69	
a_t (fm)		5.427		5.424		5.419	
$r_t = \rho(0,0)$ (fm)		1.763		1.761		1.754	

lightest long-range

short-range (repulsive core)

[a] Potential presented in Table 4.1.
[b] The σ parameters given in brackets apply to the $T = 0$ NN potential. Potential A uses 710 MeV, B and C 720 MeV for the σ mass.
[c] Meson exchange current contributions not included.

and the Λ_α are regulator masses in form factors to cut off the one-boson contributions at very short distances.

The contributions of the various mesons to the different parts of the nucleon-nucleon interaction are now given below, where

$$V_{NN}(r) = V_{central}(r) + V_{tensor}(r)\, S_{12} + V_{LS}(r)\, \vec{L}\cdot\vec{S}.$$

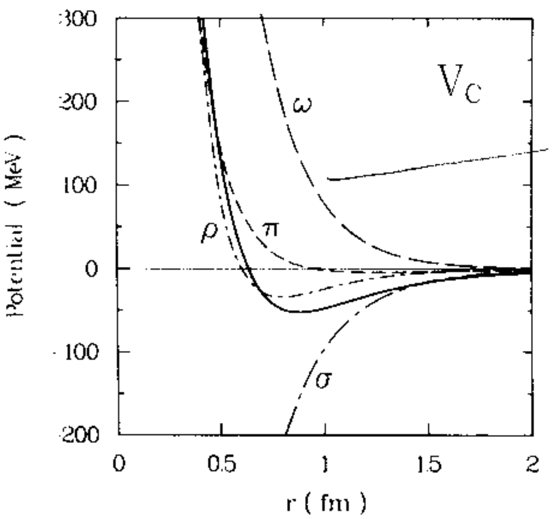

ω meson exchange generates the repulsive core!

Fig. 3.6. Contributions from single mesons to the even-singlet central potential. The solid line represents the full potential.

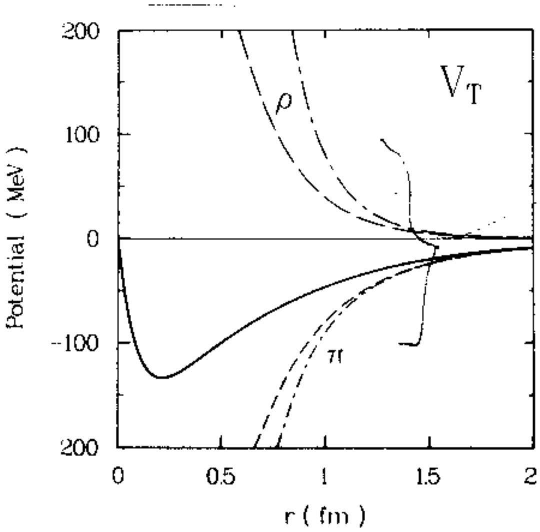

π and ρ-tensor contributions almost cancel at short distances.

Fig. 3.7. The contributions from π and ρ (dashed) to the $T = 0$ tensor potential. The solid line is the full potential. The dash-dot lines are obtained when the cutoff is omitted.

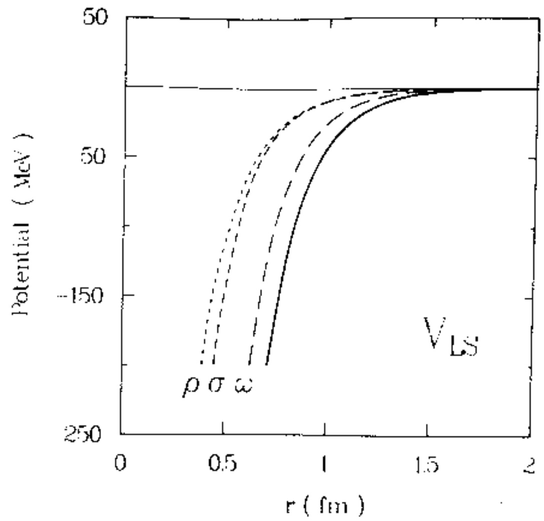

Fig. 3.8. The contributions from single mesons to the $T = 1$ spin–orbit potential, as denoted. The solid line is the full potential.

For the spin-orbit interaction, scalar and vector mesons are addition and attraction (agrees with $\vec{L}\cdot\vec{S}$ in the shell model, which is also attraction).

The renormalization group approach to the NN interaction

In addition to the Bonn potential there are several other realistic (means high precision) NN potential models, shown below. These all include the same one-pion exchange interaction at long distances, but vary in their treatment of the intermediate and short range parts

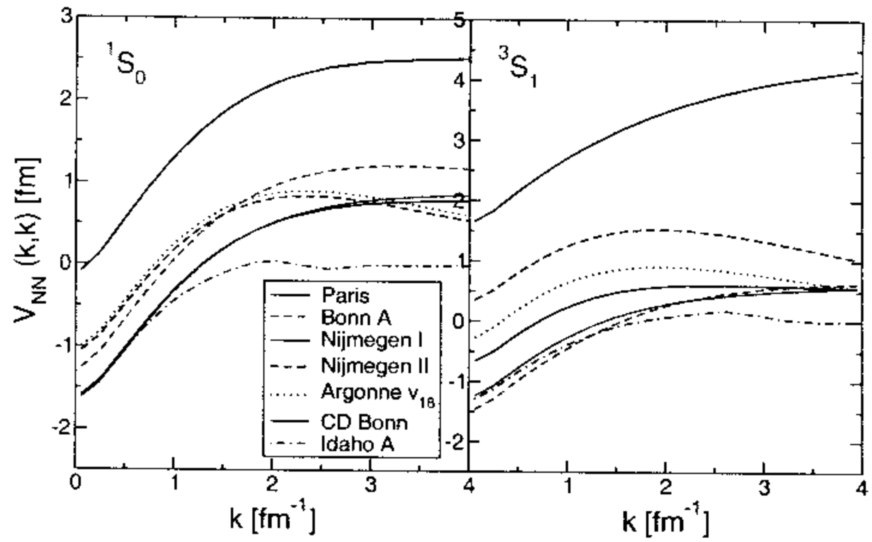

Fig. 1. Momentum-space matrix elements of $V_{\rm NN}$ for different bare potentials in the ^{1}S$_0$ and ^{3}S$_1$ channels.

The parameters of the different models are fitted to the elastic NN scattering phase shifts in partial waves for laboratory energies $E_{lab} \lesssim 350$ MeV, see page 11 of April 30, 2003 lecture. The phase shift analysis compared to on page A takes into account the world scattering data and has a $\chi^2/_{datum} \approx 1$.

A very nice feature is that the Nijmegen phase shift analysis can be accessed on-line at http://nn-online.sci.kun.nl.

Since the potential models are fitted to <u>low</u> energies below $E_{lab} \lesssim 350$ MeV, they are only constrained over relative momentum scales below a corresponding

$$k \lesssim \sqrt{\frac{m E_{lab}}{\hbar^2}} \approx 2.1 \text{ fm}^{-1}. \qquad \left(\frac{\hbar^2}{m} = 41.47 \text{ MeV fm}^2\right)$$

This corresponds to wavelengths $\lambda \sim \frac{1}{k} \approx 0.5$ fm. Therefore, the details of the potential models at short distances (high momenta) cannot be resolved by fitting to low energy data. Nevertheless, we notice that these realistic potentials have significant high momentum components, which enter in the calculation of the phase shifts through the integral term in the Lippmann-Schwinger equation.

$$\langle k' | T(E) | k \rangle = \langle k' | V | k \rangle + \frac{2}{\pi} \mathcal{P} \int_0^{\infty} q^2 dq \, \frac{\langle k' | V | q \rangle \langle q | T(E) | k \rangle}{E - q^2}$$

It would be nice, if we could simply construct a theory without such ambiguous high momentum modes by cutting off all momentum-space integrations at a cutoff $\Lambda \sim 2.1 \text{ fm}^{-1}$, then

$$\langle k' | T(E) | k \rangle = \langle k' | V | k \rangle + \frac{2}{\pi} \int_0^{\Lambda} q^2 dq \, \frac{\langle k' | V | q \rangle \langle q | T(E) | k \rangle}{E - q^2}$$

But now the phase shifts will depend on the cutoff Λ, which is not physical.

To fix this problem, we replace V by an effective potential, which cancels this cutoff dependence, i.e., V_{eff} will be cutoff-dependent. And we also show that V_{eff} only makes the so-called half-on-shell $\overset{(HoS)}{T}$ matrix for $E = k^2$ cut-off independent. It follows that all observables, which are evaluated on shell ($k = k'$, $E = k^2$) are cutoff-independent. The V_{eff} which guarantees HoS T-matrix invariance is called the <u>low momentum interaction V_{lowk}</u>. Thus, we have

$$\langle k'|T(k^2)|k\rangle = \langle k'|V_{lowk}(\Lambda)|k\rangle + \frac{2}{\pi}P\int_0^\Lambda q^2 dq \, \frac{\langle k'|V_{lowk}(\Lambda)|q\rangle}{k^2 - q^2} \, *$$

$$* \langle q|T(k^2)|k\rangle$$

with $\langle k'|T(k^2)|k\rangle$ independent of cutoff, i.e.,

$$\frac{d}{d\Lambda}\langle k'|T(k^2)|k\rangle = 0$$

This leads to a so-called <u>renormalization group (RG) equation</u>

$$\frac{d}{d\Lambda}\langle k'|V_{lowk}(\Lambda)|k\rangle = \frac{2}{\pi}\,\frac{\langle k'|V_{lowk}(\Lambda)|\Lambda\rangle\langle\Lambda|T(\Lambda^2)|k\rangle}{1 - (k/\Lambda)^2},$$

which we will derive in the next lecture.

The RG equation is an ODE and can be solved with an initial condition. For the latter, we take

$$V_{\text{low}\,k}\,(\Lambda \text{ large, typically} \sim 25\ \text{fm}^{-1}) = V_{\text{realistic}}.$$

and solve the RGE to $\Lambda = 2.1\ \text{fm}^{-1}$. Then we find (which we will discuss in detail in the next lecture)

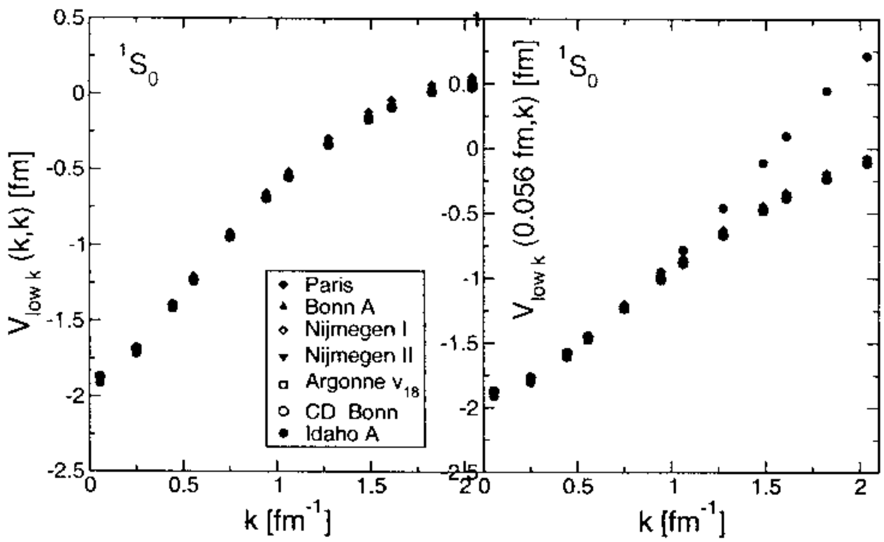

Fig. 2. Diagonal and off-diagonal momentum-space matrix elements of the $V_{\text{low k}}$ obtained from the different bare potentials in the $^1S_0$ channel for a cutoff $\Lambda = 2.1\ \text{fm}^{-1}$.

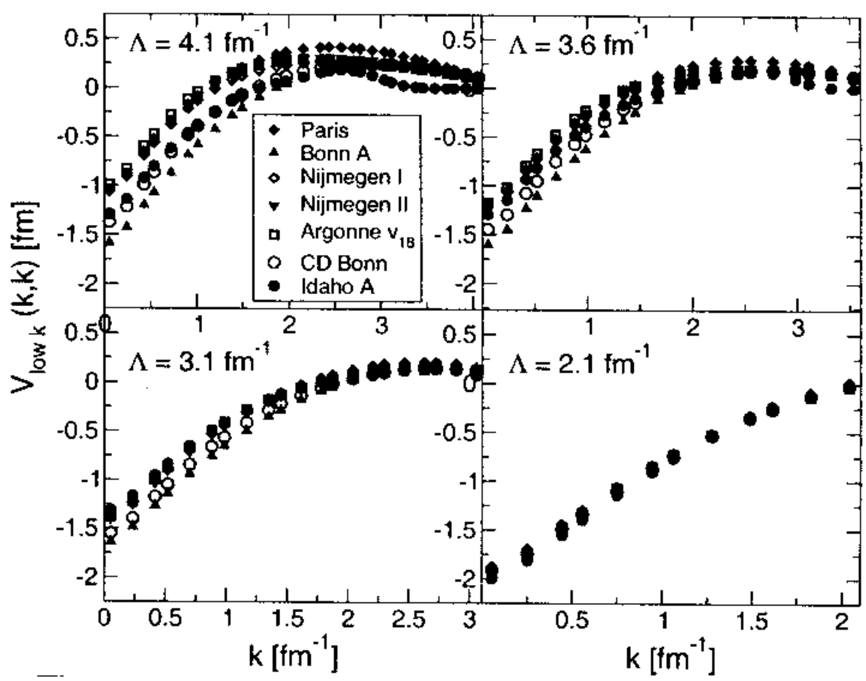

$\Rightarrow$ $V_{\text{low}\,k}$ is model independent for $\Lambda \lesssim 2.1\ \text{fm}^{-1}$ D.